

NASA TECHNICAL NOTE



NASA TN D-3348

2.1

LOAN COPY: RETURN  
AFWL (WLIL-2)  
KIRTLAND AFB, N MEX

0130619



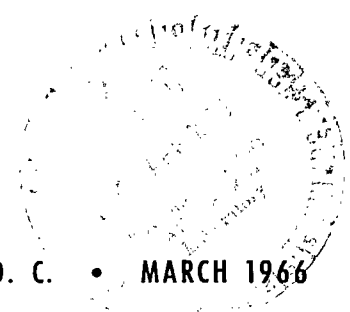
TECH LIBRARY KAFB, NM

NASA TN D-3348

GAS INGESTION AND SEALING CAPACITY  
OF HELICAL GROOVE FLUID FILM SEAL  
(VISCOSEAL) USING SODIUM AND  
WATER AS SEALED FLUIDS

*by Lawrence P. Ludwig, Thomas N. Strom, and Gordon P. Allen*  
*Lewis Research Center*  
*Cleveland, Ohio*

NATIONAL AERONAUTICS AND SPACE ADMINISTRATION • WASHINGTON, D. C. • MARCH 1966





0130619

NASA TN D-3348

GAS INGESTION AND SEALING CAPACITY OF HELICAL GROOVE  
FLUID FILM SEAL (VISCOSEAL) USING SODIUM AND WATER  
AS SEALED FLUIDS

By Lawrence P. Ludwig, Thomas N. Strom, and Gordon P. Allen

Lewis Research Center  
Cleveland, Ohio

NATIONAL AERONAUTICS AND SPACE ADMINISTRATION

---

For sale by the Clearinghouse for Federal Scientific and Technical Information  
Springfield, Virginia 22151 – Price \$0.35

GAS INGESTION AND SEALING CAPACITY OF HELICAL GROOVE FLUID  
FILM SEAL (VISCOSEAL) USING SODIUM AND WATER AS  
SEALED FLUIDS

by Lawrence P. Ludwig, Thomas N. Strom, and Gordon P. Allen

Lewis Research Center

SUMMARY

An experimental investigation was conducted on gas ingestion and sealing capacity (expressed as a dimensionless sealing parameter,  $\lambda G$ ) of viscoseals using water and liquid sodium as the sealed fluids. The investigation covered a Reynolds number range of 2100 to 60 500. Results disclosed that a helically grooved rotor viscoseal (smooth bore housing) has increasing gas ingestion rates with increasing Reynolds number when the viscoseal liquid interface becomes unstable. Helically grooved housing viscoseals (smooth rotors) showed no gas ingestion when sealing sodium (Reynolds numbers from 10 400 to 37 200); when sealing water, gas ingestion occurred only within a specific range of Reynolds numbers (2300 to 8400). Secondary grooves on viscoseal land areas improved sealing capacity and reduced power absorption. Sodium was sealed at 149° to 329° C (300° to 625° F) without measurable liquid loss for operational periods up to 8 hours.

INTRODUCTION

Long-life, high-reliability shaft seals, having near zero leakage rates are required for rotating-shaft electric power generation systems utilizing alkali metals (refs. 1 and 2). Other alkali-metal shaft-seal applications are found in centrifugal pumps that handle liquid metals (ref. 3) and in extreme-temperature (1000° F) hydraulic (liquid metal) systems (ref. 4). The helical groove fluid film seal (hereinafter called the viscoseal) is a potentially useful liquid metal seal (or component of a seal system) because the absence of solid surfaces in sliding contact provides inherent long life and high reliability.

Gas ingestion from the low-pressure to the high-pressure end of the seal is reported to have occurred when sealing potassium (ref. 1) and when sealing water (data obtained by William K. Stair, Univ. of Tenn.). Although this gas ingestion characteristic may present no problem with a vacuum on the low-pressure end, it is highly undesirable in other potential applications because of contamination and/or detrimental effect on sealing capacity. Experimental or theoretical data on gas ingestion by viscoseals are not available in the literature.

Reference 5 reports that in attempting to seal a liquid, the viscoseals (combining helical grooves in rotor and housing) worked on an air-liquid emulsion, and reference 6 reports that viscoseals (helical grooves on shaft) operate with a mixture of oil and gas. This mode of operation could be due to gas ingestion. Leakage observations reported in reference 7 on "seal breakdown" and in reference 1 on "secondary leakage" could result from gas ingestion into a closed cavity.

The theoretical viscoseal pressure generation has been derived by several investigators (refs. 7 to 12). These derivations, which apply only to the slow viscous flow regime, are based on a homogeneous liquid (no gas bubbles). No viscoseal analysis exists for the flow regime in which inertia forces are significant. Experimental data on sealing of oils and water in regimes defined as turbulent are limited (refs. 1 and 7), and limited data on viscoseal operation in alkali metals are available in reference 1.

This study obtains experimental data on viscoseal gas ingestion and sealing capacity (expressed as a dimensionless sealing parameter,  $\lambda G$ ) with water and liquid sodium as sealed fluids. Studies of the gas ingestion process, with water as the sealed fluid, were made by using a transparent viscoseal housing to permit visual observation of the flow regimes. Sealing capacity and gas ingestion rates were determined for liquid sodium within a Reynolds number range of 10 400 to 60 500. Different viscoseal geometries were evaluated by using the geometry near the optimum (derived in ref. 9) as a basis of comparison.

#### APPARATUS AND PROCEDURE

The helically grooved housing-smooth rotor combination (hereinafter called grooved housing) is shown in figure 1, and the helically grooved shaft-smooth bore housing combination (hereinafter called grooved rotor) is shown in figure 2. Both combinations were evaluated in water and in liquid sodium.

Figures 1 and 2 show typical experimental setups applied to seal water and sodium, respectively. The rotors of the viscoseals are attached to the power input shaft, which is driven by a variable-speed electric drive and a stepup transmission. A magnetic pickup monitors the shaft speed.

In studies on sealing water, the water pressure and flow to the pressurized cavity (at the viscoseal high-pressure end) were controlled by throttling valves on the inlet and outlet water lines. This arrangement provided temperature control of the sealed fluid. A transparent housing permitted visual observations on the gas quantity in the pressurized cavity and on the gas ingestion process within the viscoseal. A transparent outlet line permitted observations on the rate of gas flow out of the pressurized cavity; and, in studies on grooved rotors, a stroboscope permitted observations of the gas ingestion process in the rotating grooves. In the grooved housing (fig. 3) pressure taps were located at groove edges and at midland and midgroove positions in a line parallel to the rotor centerline. Pressure taps were also located near both edges

along one groove. Two sets of four pressure taps ( $90^\circ$  apart) were used to align the housing with respect to the rotor within 0.00102 centimeter (0.0004 in.). Thermocouples were located flush with the bore and groove root in a line parallel to the rotor centerline and at each midgroove and midland position. The smooth-bore housing also had pressure taps and thermocouples in a line parallel to the rotor centerline.

In studies on sealing sodium the temperature was maintained by a furnace (resistance heaters) surrounding the viscoseal housing (fig. 2). The temperature was monitored by thermocouples attached to the seal housing outer diameter and by one thermocouple submerged in the sodium in the pressurized cavity.

Figure 4 is a diagrammatic sketch of the experimental apparatus used for evaluating viscoseals in sodium. The enclosure surrounding the viscoseal assembly is pressurized with argon (after prior evacuation) to slightly above ambient to ensure exclusion of air. Prior to the introduction of liquid sodium, the input shaft is set at some fixed speed. Sodium is introduced by pressurizing the reservoir and venting the leak detector tank. The sodium first fills the pressurized cavity (viscoseal high-pressure end) and then is allowed to fill the leak detector tank to a predetermined level. The tank float displacement is monitored by recording the differential transformer output that is produced by the transformer core attached to the top of the float. Thermocouples placed at different levels in the tank provide calibration during the filling process.

By holding the reservoir temperature at  $104^\circ\text{C}$  ( $220^\circ\text{F}$ ), a low degree (10 ppm) of oxide solubility was maintained. The 20-micron filter (stainless steel) inside the tank provides  $104^\circ\text{C}$  filtration. A second filter external to the reservoir ( $5\ \mu$ ) provides additional filtering at approximately  $149^\circ\text{C}$  ( $300^\circ\text{F}$ ).

Sodium is partially removed from the system by pressurizing the leak detector and forcing the sodium back into the reservoir. By alternately filling the system and then partially returning the sodium to the reservoir, the sodium can be recirculated and refiltered. This recirculation provides a hot flush or cleaning action on the viscoseal assembly before a run. (All transfer lines and the test section are held at  $149^\circ$  to  $260^\circ\text{C}$  ( $300^\circ$  to  $500^\circ\text{F}$ ) during this recirculation process.) For all sodium studies the leak detector tank was held at  $149^\circ\text{C}$  ( $300^\circ\text{F}$ ), and any seal leakage resulted in a drop of liquid level and float position. Gas ingestion into the pressurized cavity was indicated by a rise in sodium level in the leak detector. The sealed pressure is the pressure on the leak detector with corrections for the enclosure pressure.

Sealing capacity, when sealing sodium, was obtained by increasing cavity pressure until the leak detector indicated leakage. Line thermocouple readings were also found to be sensitive leak indicators.

Viscoseal geometries employed in this evaluation are shown in table I. The geometry near the optimum (derived in ref. 9) was taken as the basis for comparison, and is listed in the first row of table I as geometry 1. Secondary grooves were added to the lands of this basic geometry to form the second geom-

etry evaluated. For the third geometry, a ratio of groove to land width of 1.90 was selected; and for the fourth geometry, secondary grooves were added to geometry 3. Geometry 5 is the internally grooved housing having the same groove dimensions as geometry 1. The rotor outer diameters were 5.062 centimeters (1.993 in.), and the housing bores were 5.082 centimeters (2.001 in.).

## RESULTS AND DISCUSSION

### Viscoseal Theory

For slow viscous laminar flow the theoretical pressure generation equation (ref. 13) is

$$\frac{\Delta P}{L} = \frac{6U\mu G}{c^2}$$

where

$\Delta P$  differential pressure between high- and low-pressure end of seal

$L$  calculated wetted-seal length

$U$  rotor peripheral velocity

$\mu$  absolute viscosity

$G$  function of helical geometry, dimensionless

$c$  radial clearance

To correlate theory and experiment, the preceding equation is modified by a factor defined as the sealing coefficient  $\lambda$ , which includes effects of inertia, eccentricity, machining variations, turbulence, and gas ingestion. It is useful to write the preceding equation in the form

$$\lambda G = \frac{c^2 \Delta P}{6\mu UL}$$

in which the dimensionless sealing parameter  $\lambda G$  is a measure of sealing capacity and embodies the geometry factor  $G$  and the sealing coefficient  $\lambda$ . As  $\lambda G$  increases, the sealing capacity increases.

### Observations When Sealing Water

Grooved housing. - The series of photographs in figure 5 shows the gas ingestion process when sealing water with a grooved housing and smooth outer diameter rotor. At a Reynolds number of 2100 (2000 rpm), no gas ingestion is evident, the water film is clear, the interface is stable, and the scavenging length is nonwetted. The Reynolds number for this study is defined as

$$Re = \frac{U(c + h)}{\eta} = \frac{\rho U(c + h)}{\mu}$$

where

$h$  groove depth

$\eta$  kinematic viscosity

$\rho$  density

$\mu$  absolute viscosity

At  $Re = 3100$  (3000 rpm) the film had large gas pockets, gas was ingested as evidenced by air bubbles passing out of the transparent vent line, and the sealing capacity (parameter,  $\lambda G$ ) was lower than that at 2100 (2000 rpm). Various degrees of gas ingestion and film rupture are evident for  $Re = 4200$  (4000 rpm) to 7300 (7000 rpm). At  $Re = 8400$  (8000 rpm), no detectable gas ingestion rate was evident, and gas ingestion was not detectable from  $Re = 8400$  (8000 rpm) to the highest speed evaluated, which gave  $Re = 13\ 000$  (12 000 rpm). At  $Re = 8400$  and above the seal wetted length had two distinct regions (fig. 5(f)): a gas-liquid region and a region of homogeneous liquid at the high-pressure end. Between  $Re = 2300$  and 7300, figures 5(b) to (e) show that the entire wetted seal length contains a mixture of liquid and gas.

Between  $Re = 4200$  and 7300, it was observed that the bubbles size progressively decreased when moving from the low-pressure end to the high-pressure end. It is probable that with longer seal lengths the corresponding higher pressures would reduce the bubble size sufficiently to allow escape over the lands, and thus gas ingestion would be eliminated. It was observed that concentricity of rotor and housing markedly affect gas ingestion occurrence.

Grooved rotor. - In a series of visual observations using a grooved rotor, the gas ingestion started at  $Re = 2300$  and increased in rate with increasing Reynolds number (maximum investigated,  $Re = 13\ 000$ ). Below  $Re = 2300$  the liquid-to-gas interface was stable and no gas ingestion occurred.

Gas ingestion mechanism. - These observed gas ingestion characteristics of the grooved rotor and the grooved housing are illustrated in figure 6. The probable mechanism producing the difference between the gas ingestion process of the grooved rotor as compared with that of the grooved housing is illustrated in figure 7. For the grooved housing, when the centrifuge action on the liquid becomes great enough, the gas bubbles are displaced to the rotor surface and pass over the lands. Therefore, the bubbles are not pumped to the high-pressure end. For the grooved rotor, the centrifugal action on the liquid forces the gas bubbles into the grooves; therefore, the bubbles are pumped to the high-pressure end of the seal.

When a viscoseal is ingesting gas, the axial pressure gradient is nonlinear and increases as the liquid-to-gas volume ratio increases in the direction toward the high-pressure end. For no gas ingestion, the axial pressure gradi-

ents are linear as shown in figure 8, which contains data on sealing oil from reference 13. As shown in figure 9, gas ingestion results in nonlinear pressure gradients (increasing slope with increasing liquid-gas volume), which are significantly different from the gradients shown in figure 8.

Leak rate. - In both viscoseal combinations (grooved housing and grooved rotor) water was sealed, with no detectable leakage. It was observed that, although gas ingestion reduced the sealing coefficient  $\lambda$ , effective sealing of the water was maintained.

### Results of Sodium Sealing Studies

Grooved housing. - In sealing sodium, data showed that the grooved housing did not ingest gas (fig. 10) for concentric alignment (0.0012 cm F.I.R.) over the range investigated ( $Re = 10\ 400$  to  $60\ 500$ ) and for pressures ranging from 1.4 to 68.9 newtons per square centimeter (2 to 100 psig). The sensitivity of the leak detector to measure gas ingestion rate was estimated to be 0.50 cubic centimeter per hour. It was observed that nonconcentricity leads to gas ingestion, but this situation was not investigated.

Grooved rotor. - The grooved rotor started to ingest gas at  $Re \approx 12\ 000$ , and the rate increased with increasing Reynolds number, as shown in figure 10. This ingestion characteristic is similar to that observed when sealing water with the grooved rotor.

Gas ingestion into closed cavity. - In sealing sodium, gas ingestion was readily observed by monitoring the liquid level in the leak detector. As shown in figure 11, a straight line on the oscillograph paper indicated no gas ingestion, no leakage, and thermal equilibrium. When gas ingestion occurred, the liquid level line showed an upward trend, the slope of which is the ingestion rate. As gas ingestion proceeds, the gas bubble in the pressurized cavity increases in size (fig. 11(a)), and when the size increases to the rotor outer diameter, the gas blows back out the annulus formed by the rotor and housing. This causes a decrease in bubble size and a sharp drop in the leak detector readout trace. If the interface is far enough away from the seal low-pressure end, the liquid will be scavenged back within the nonwetted length, and no loss of liquid will occur. The ingestion process will begin again and the net result is a saw-toothed trace, each sharp drop indicating gas blowback. If the interface is sufficiently close to the seal end, liquid loss will occur, and the leak detector readout will show a saw-toothed profile trace with a downward trend, which represents a liquid loss at each blowout (fig. 11(c)). This latter action may be the "seal breakdown" phenomenon reported in reference 7 and the "secondary leakage" phenomenon reported in reference 1. (In sealing water, the repeating bubble growth and subsequent seal blowout was visually observed by means of a transparent housing.)

Sealing capacity. - The grooved housing had a higher sealing capacity (higher sealing parameter,  $\lambda G$ ) than the grooved rotor. The comparison is given in figure 12, which gives the sealing parameter  $\lambda G$  as a function of Reynolds number. This parameter  $\lambda G$  is the same as the sealing coefficient given in references 1 and 7 and the inverse of the sealing coefficient given in refer-



ence 12. The difference between the value of  $\lambda G$  for the grooved housing and the value for the grooved rotor was attributed to the difference in gas ingestion characteristics. The grooved rotor operates with a gas-liquid mixture along the full wetted length similar to that shown in figures 5(b) to (e); the grooved housing operates with a homogeneous liquid at the high-pressure end of the seal and a gas-liquid mixture at the low-pressure end similar to that shown in figure 5(f).

Figures 13(a) and (b) show the sealing parameter  $\lambda G$  as a function of Reynolds number for groove configurations of five- and ten-helix starts (see table I) with and without secondary grooves on the lands. In both cases, a higher sealing coefficient was obtained through the use of secondary grooves. Secondary grooves also operate at lower power absorption levels for equal sealing capacity, as was determined by the amount of heating power required to maintain operating temperature. This lower power absorption is due to less land area as compared with the land area of the seals without secondary grooves.

Sodium was sealed for pressures ranging from 1.4 to 68.9 newtons per square centimeter (2 to 100 psig) without detectable leakage loss. The operating range was within Reynolds numbers of 10 400 to 60 500, and the fluid temperature was in the range 149° to 329° C (300° to 625° F). The maximum length of any one run was 8 hours and accumulated testing time amounted to 50 hours for 10 runs. The oxygen content of the sodium for the 10 runs varied between 50 to 95 parts per million, as determined by the analytical method described in reference 14.

## SUMMARY OF RESULTS

Visual observations and experimental evaluation of viscoseal assemblies with water (Reynolds numbers of 2100 to 13 000) and sodium (Reynolds numbers of 10 400 to 60 500) as sealed fluids disclosed the following:

1. Gas ingestion characteristics were fundamentally different for the helically grooved rotor-smooth bore housing combination as compared with the helically grooved housing-smooth rotor combination. In the grooved housing-smooth rotor combination, centrifugal action worked to hold the gas bubbles out of the groove; thus the bubbles tended to escape over the lands rather than be pumped into the seal high-pressure end. In the grooved rotor-smooth bore housing combination centrifugal action forced the gas bubbles into the rotor grooves; thus the gas bubbles were pumped into the seal high-pressure end.

2. In sealing sodium, the grooved housing-smooth rotor combination had no detectable gas ingestion rate, but the grooved rotor-smooth bore housing combination showed increasing gas ingestion with increasing Reynolds number.

3. No gas ingestion occurred when sealing water with either the grooved rotor-smooth bore housing or the grooved housing-smooth rotor viscoseal when the liquid interface was stable (below Reynolds number of 2300).

4. In sealing sodium, the grooved housing-smooth rotor combination produced a higher sealing capacity (higher sealing parameter) than the grooved rotor-smooth bore housing combination. This was attributed to the presence of gas ingestion in the case of the grooved rotor.

5. Sealing, with no detectable sodium leakage rate, was obtained for short operational periods (maximum length of continuous evaluation was 8 hours) over a pressure range of 1.4 to 68.9 newtons per square centimeter (2 to 100 lb force/sq in. gage) and at sodium temperatures of 149° to 329° C (300° to 625° F).

6. Secondary grooves on land rotor surfaces produced higher sealing capacities (higher sealing parameter) and lower power absorption as compared to rotors without secondary grooves.

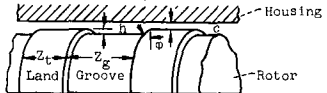
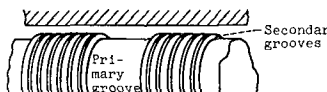
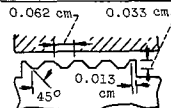
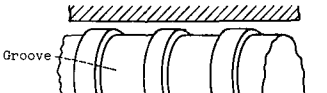
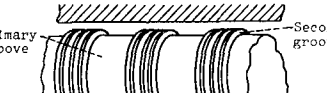
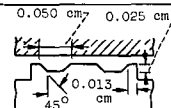
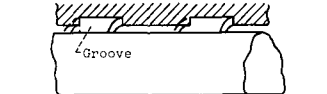
Lewis Research Center,  
National Aeronautics and Space Administration,  
Cleveland, Ohio, December 7, 1965.

#### REFERENCES

1. King, Alan E.: Screw Type Shaft Seals for Potassium Lubricated Generators. IEEE Trans. on Aerospace, vol. AS-3, June 1965, Supplement, pp. 471-479.
2. Gruntz, Robert D.; and Rackley, Ray A.: Snap 50/Spur Power Conversion System-Objectives, Current Status and Lunar Applications. Paper No. 650321, SAE, May 1965.
3. Wood, G. M.; Manfredi, D. V.; and Cygnor, J. E.: Centrifugal Types of Dynamic Shaft Seals. Paper No. 63-WA-167, ASME, Nov. 1963.
4. Billet, A. B.: Hydraulic Sealing in Space Environments. Proceedings of the Second International Conference on Fluid Sealing, B. S. Nau, H. S. Stephens, and D. E. Turnbull, eds., British Hydromechanics Research Association, Harlow, Essex, England, 1964, pp. C2-17-C2-36.
5. Golubiev, A. I.: Studies on Seals for Rotating Shafts of High-Pressure Pumps. Wear, vol. 8, no. 4 July/Aug. 1965, pp. 270-288.
6. Holan, Karel: Sealing in Engineering. Proceedings of the Second International Conference on Fluid Sealing, B. S. Nau, H. S. Stephens, and D. E. Turnbull eds., British Hydromechanics Research Association, Harlow, Essex, England, 1964, pp. E5-73-E5-88.
7. McGrew, J. M.; and McHugh, J. D.: Analysis and Test of the Screw Seal in Laminar and Turbulent Operation. Paper 64-IJBS-7, ASME Apr. 1964.
8. Boon, E. F.; and Tal, S. E.: Hydrodynamic Seal for Rotating Shafts. DEG. Inf. Ser. 13, United Kingdom Atomic Energy Authority, 1961.

9. Zotov, V. A.: Research on Helical Groove Seals. Russ. Eng. J., vol. 10, Oct. 1959, pp. 3-7.
10. Asanuma, T.: Studies on the Sealing Action of Viscous Fluids. Paper No. A3 presented at the First International Conference on Fluid Sealing, Cranfield, England. British Hydromechanics Research Association, Harlow, Essex, England, Apr. 1961.
11. Muijderman, E. A.: Spiral Groove Bearings. Philips Res. Rept. Suppl., no. 2, 1964.
12. Stair, William K.: Analysis of the Visco Seal. Rep. No. ME 65-587-2, University of Tennessee, Jan. 18, 1965.
13. Ludwig, Lawrence P.; Strom, Thomas N.; and Allen, Gordon P.: Experimental Study of End Effect and Pressure Patterns in Helical Groove Fluid Film Seal (Viscoseal). NASA TN D-3096, 1965.
14. Kuivinen, David E.: Determination of Oxygen in Liquid Alkali Metals by the Mercury Amalgamation Method. Paper presented at the Nineteenth Meeting, Chemical Rocket Propulsion Group (St. Paul, Minn.), July-Aug., 1963.

TABLE I. - VISCOSEAL GEOMETRIES

Geometry	Configuration	Primary grooves							Secondary grooves		
		Groove width, $Z_g$ , cm	Land width, $Z_t$ , cm	Ratio of groove to land width, $Z_g/Z_t$	Groove depth, $h$ , cm	Radial clearance, $c$ , cm	Primary helix angle, $\phi$ , deg	Number of helix starts	Number of helix starts per land	Secondary helix angle, $\phi_s$ , deg	Cross section through land
a <sub>1</sub>		0.480 (0.190 in.)	0.33 (0.130 in.)	1.5	0.032 (0.013 in.)	0.010 (0.004 in.)	14.5	5	0	----	
2 (Geometry 1 plus secondary grooves)		0.480 (0.190 in.)	0.33 (0.130 in.)	1.5	0.032 (0.013 in.)	0.010 (0.004 in.)	14.5	5	4	14.5	
3		0.266 (0.105 in.)	0.14 (0.055 in.)	1.9	0.032 (0.013 in.)	0.010 (0.004 in.)	14.5	10	0	----	
4 (Geometry 3 plus secondary grooves)		0.266 (0.105 in.)	0.0140 (0.055 in.)	1.9	0.032 (0.013 in.)	0.010 (0.004 in.)	14.5	10	2	14.5	
5		0.480 (0.190 in.)	0.033 (0.130 in.)	1.5	0.032 (0.013 in.)	0.010 (0.004 in.)	14.5	5	0	----	

<sup>a</sup>Used as base line.

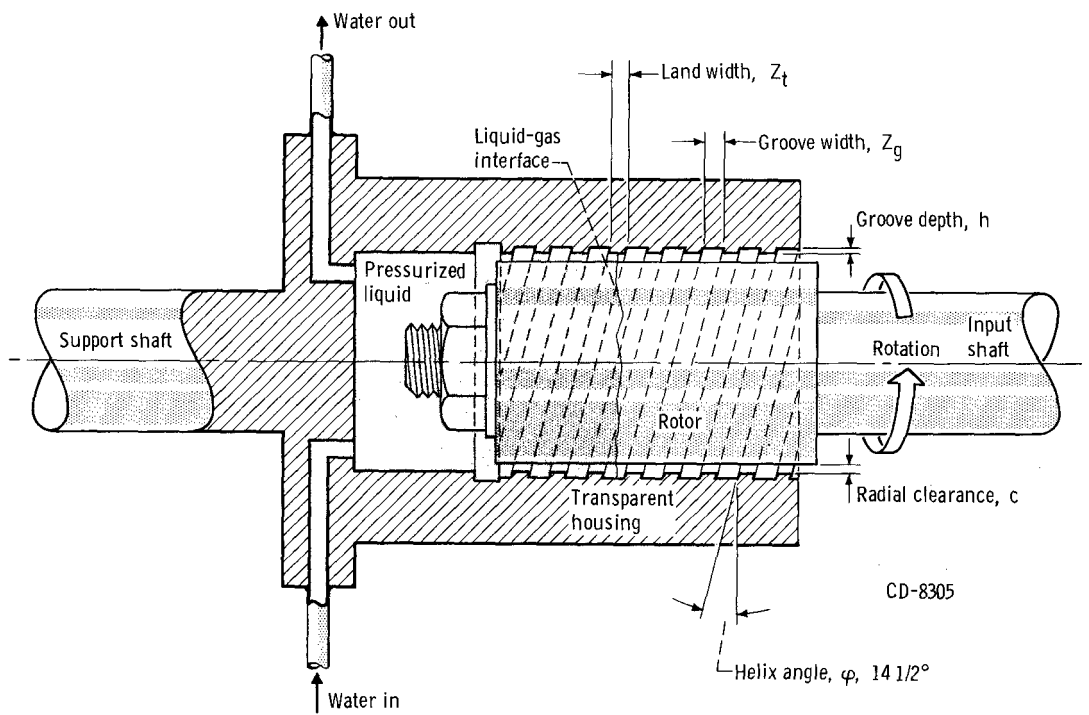


Figure 1. - Internal grooved housing viscoseal used with water.

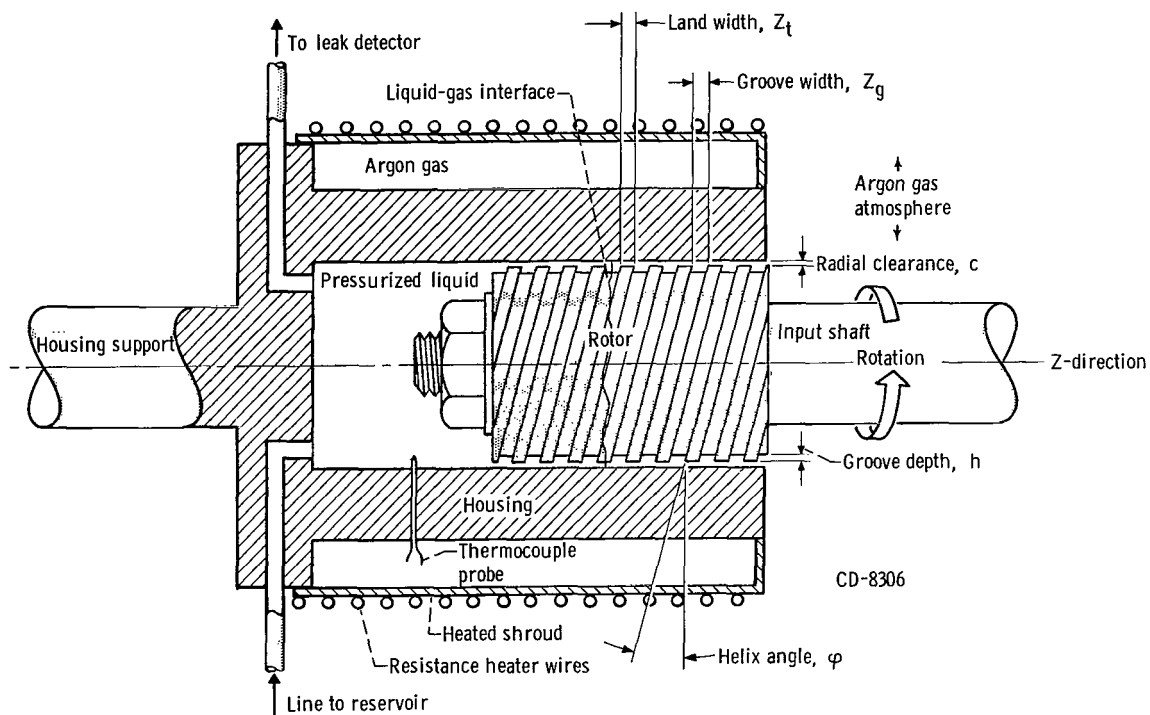


Figure 2. - Grooved rotor viscoseal used to seal sodium.

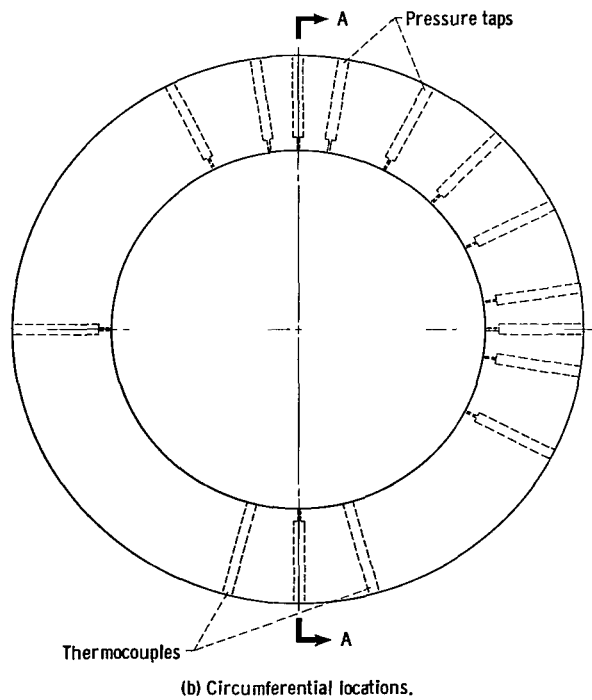
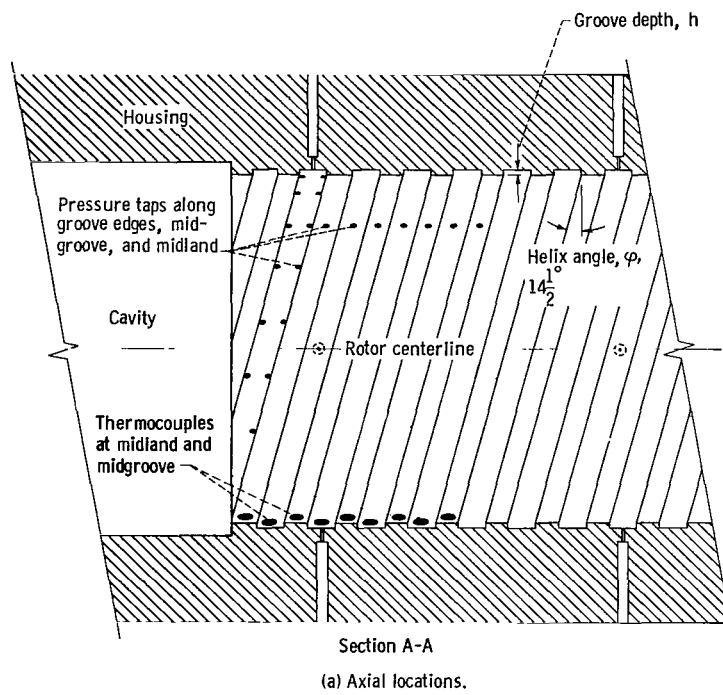


Figure 3. - Pressure tap and thermocouple locations.

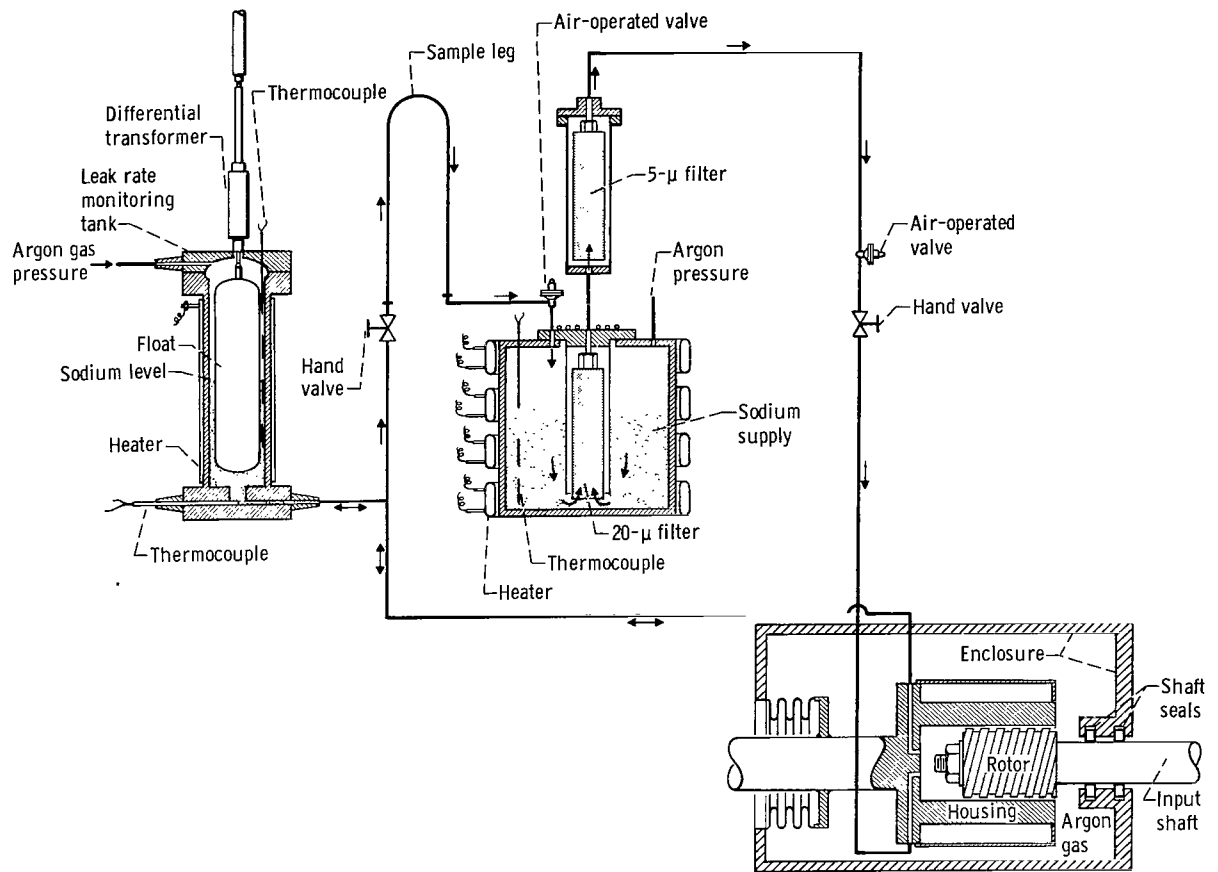
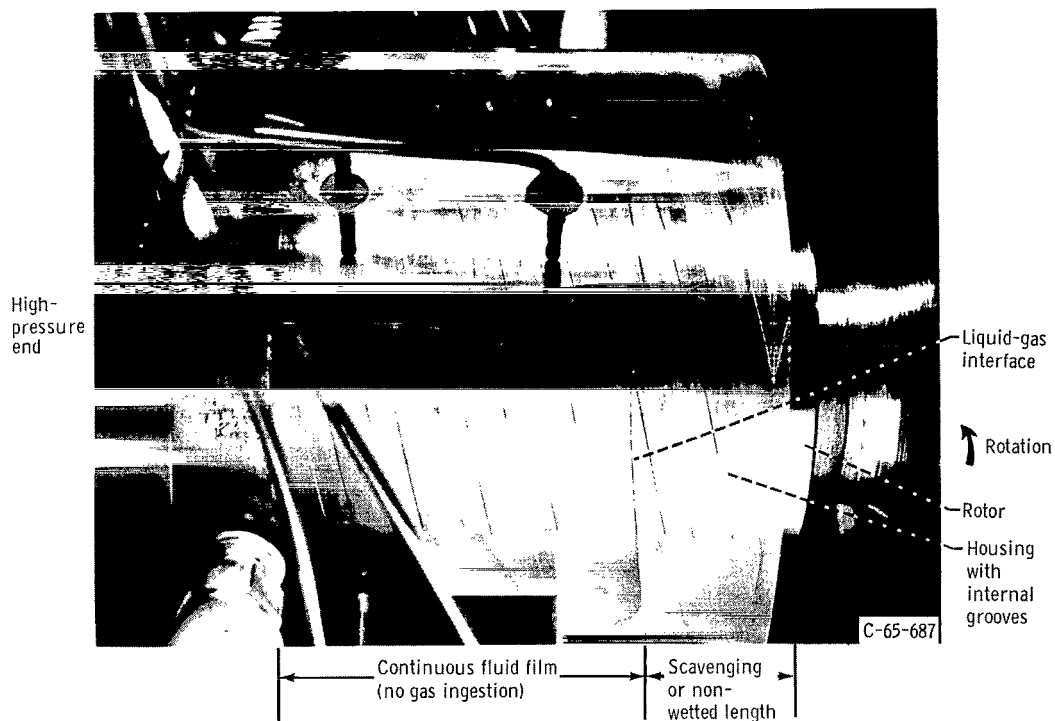


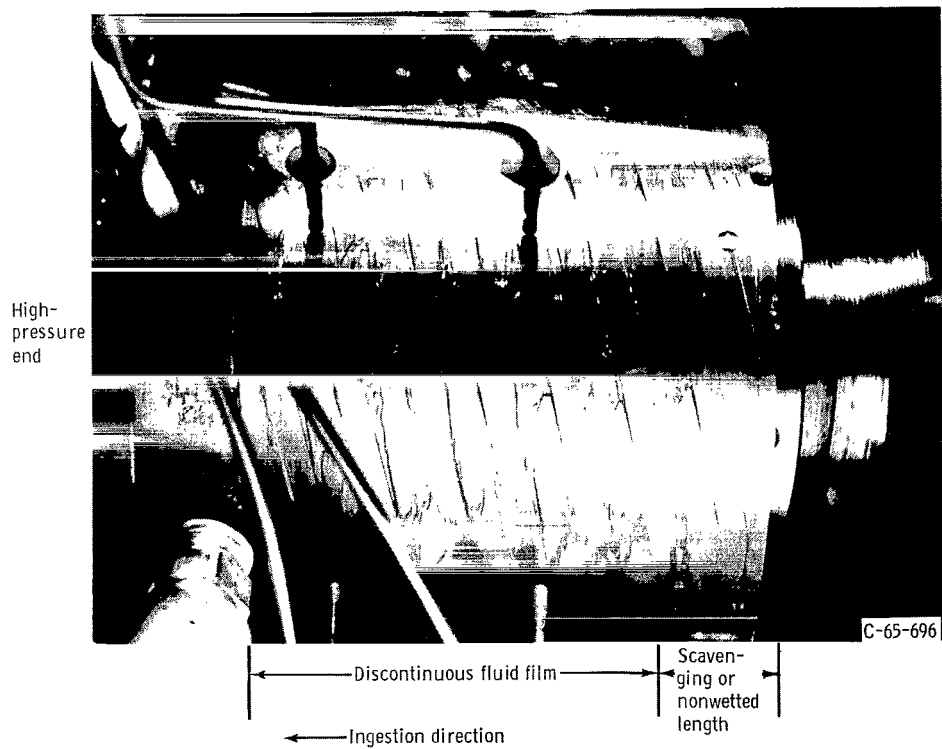
Figure 4. - Sodium supply system.

CD-8307





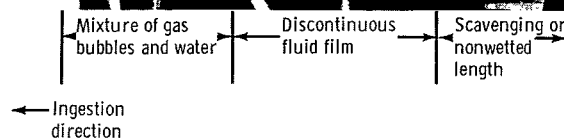
(a) Reynolds number, 2100 (2000 rpm).



(b) Reynolds number, 3100 (3000 rpm).

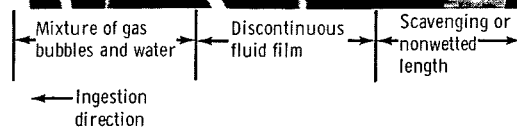
Figure 5. - Grooved housing viscoseal operation when sealing water.

High-  
pressure  
end



(c) Reynolds number, 4200 (4000 rpm).

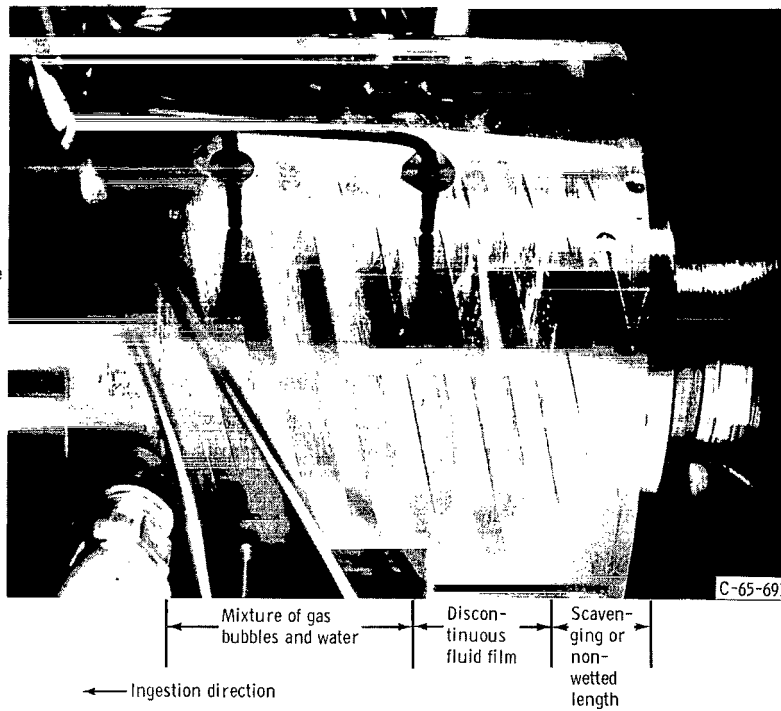
High-  
pressure  
end



(d) Reynolds number, 5300 (5000 rpm).

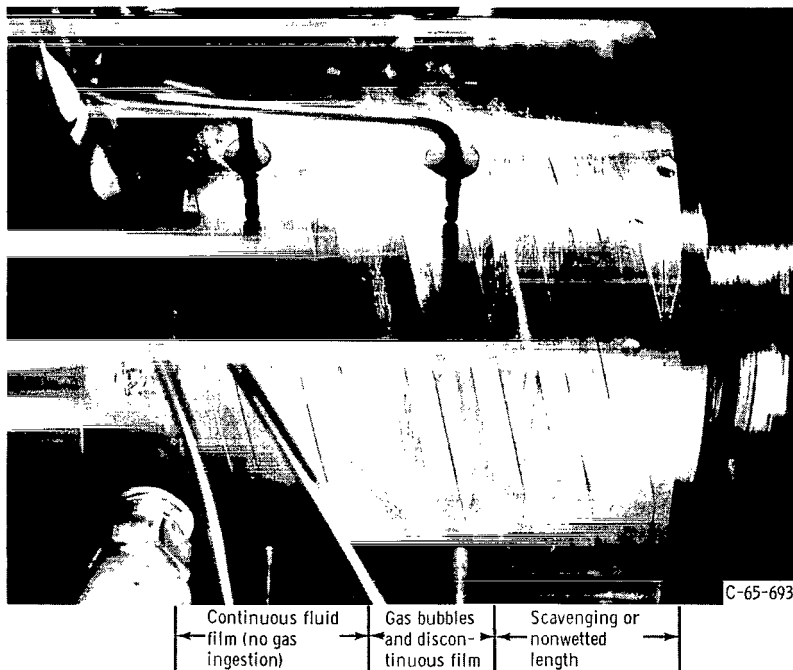
Figure 5. - Continued.

High-  
pressure  
end



(e) Reynolds number, 6300 (6000 rpm).

High-  
pressure  
end



(f) Reynolds number, 8400 (8000 rpm).

Figure 5. - Concluded.

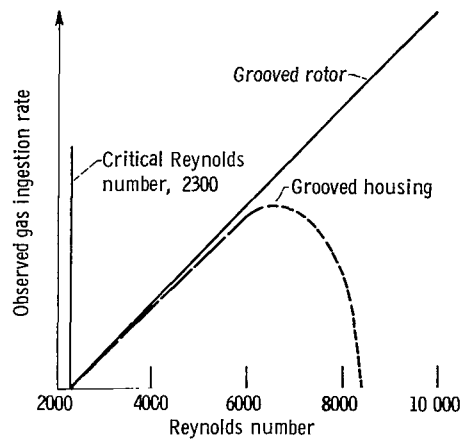


Figure 6. - Comparison of observed gas ingestion when sealing water for grooved housing and grooved rotor viscoseals.

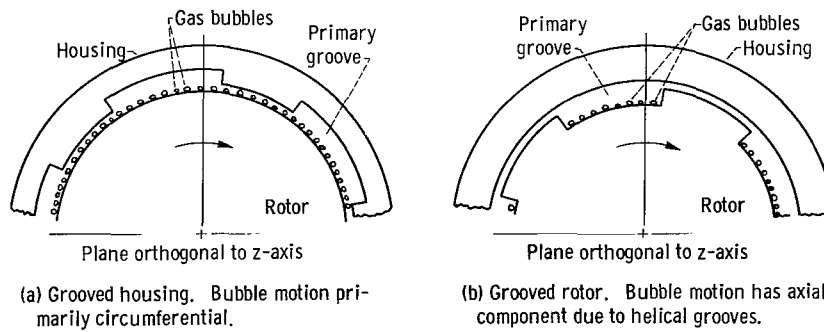


Figure 7. - Gas ingestion mechanisms of grooved housing compared with grooved rotor viscoseal.

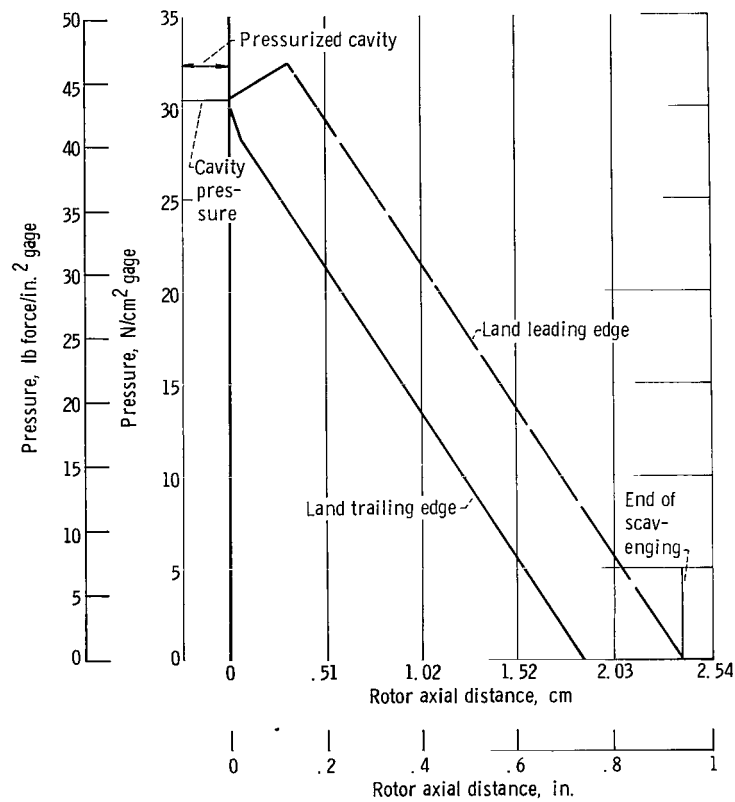


Figure 8. - Pressure as function of axial length without gas ingestion for grooved rotor at Reynolds number of 57. Sealed fluid, oil (ref, 14).

High-  
pressure  
end



← Gas ingestion direction and  
increasing liquid-gas density

No leakage at  
low-pressure  
end

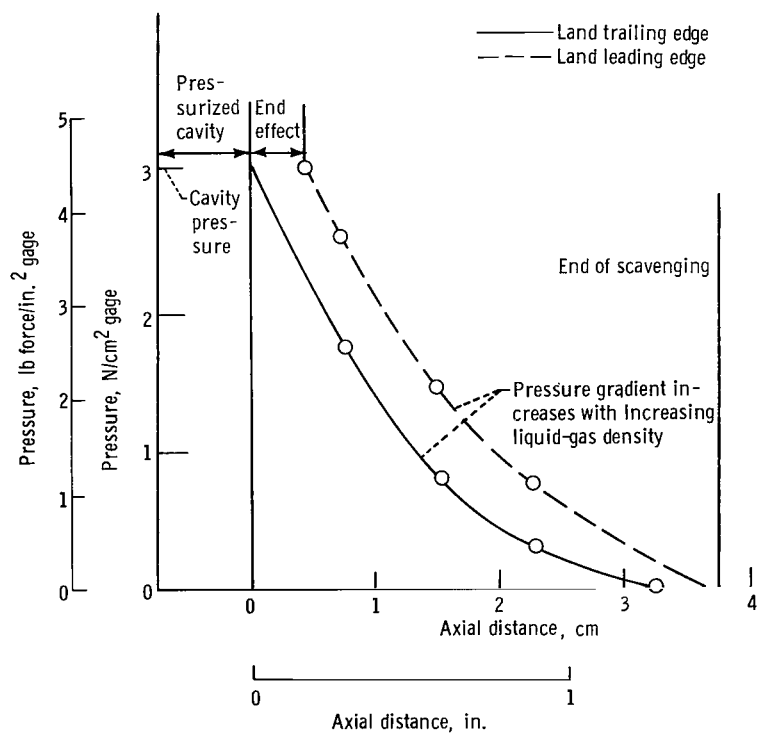


Figure 9. - Pressure as function of axial length with gas ingestion for grooved rotor. Sealed fluid, water.

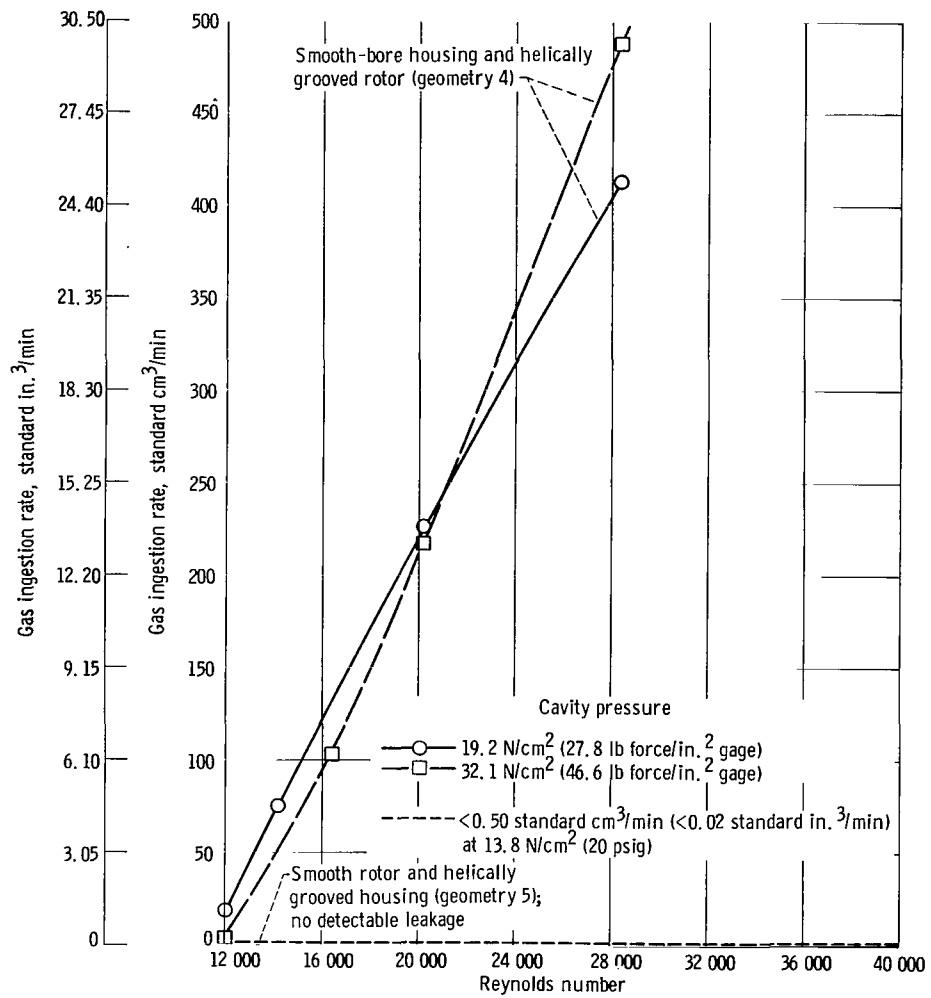
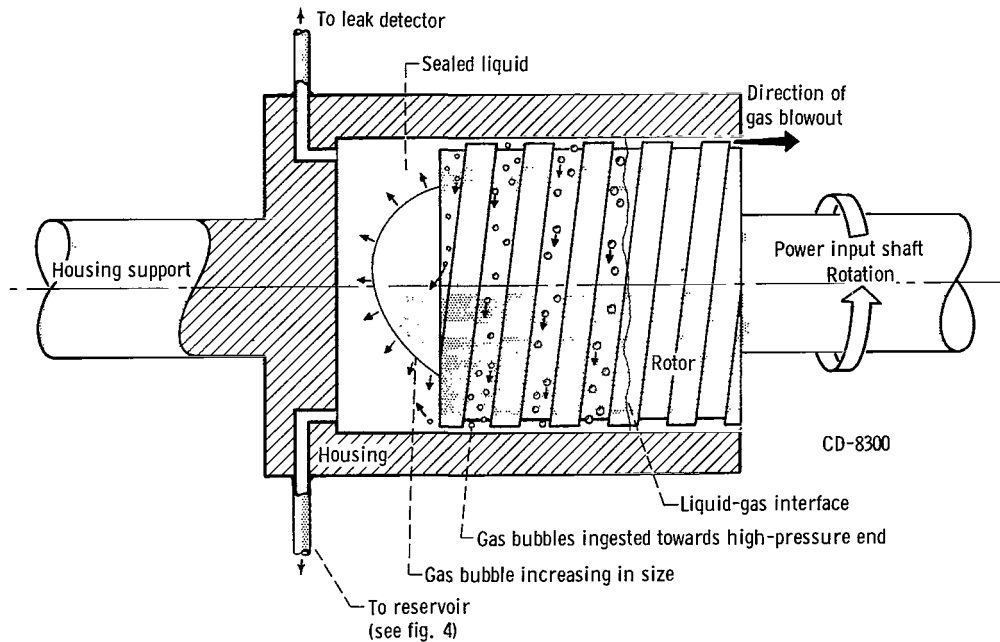
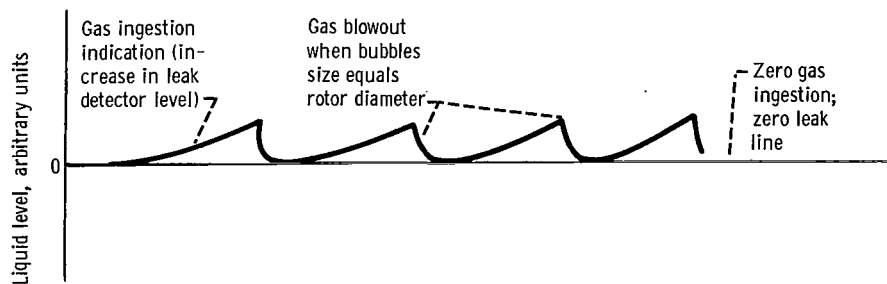


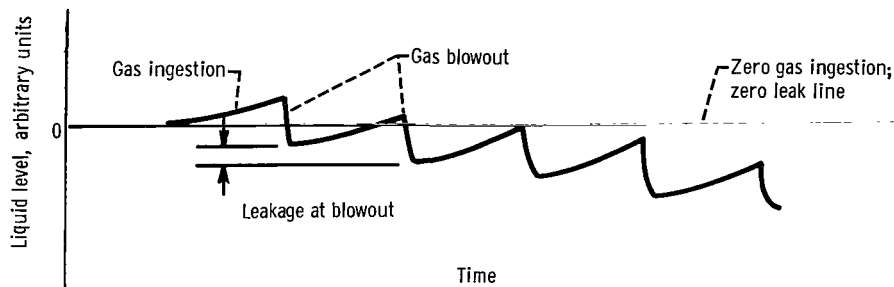
Figure 10. - Gas ingestion rate when sealing liquid sodium at 400° F.



(a) Mechanism involved in gas ingestion into pressurized cavity.



(b) Schematic liquid level oscillograph trace for repeated cycles of gas ingestion, subsequent gas blowout, and no liquid leakage at blowout.



(c) Schematic liquid level oscillograph trace for repeated cycles of gas ingestion, subsequent gas blowout, and liquid leakage at blowout.

Figure 11. - Gas ingestion into closed cavity.



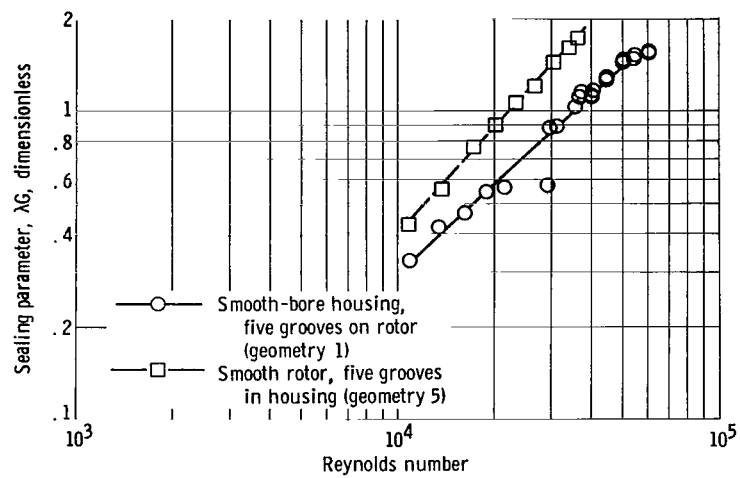


Figure 12. - Comparison of sealing parameters for grooved rotor and housing operating in sodium. Sodium temperature, 165° to 335° C (329° to 635° F).

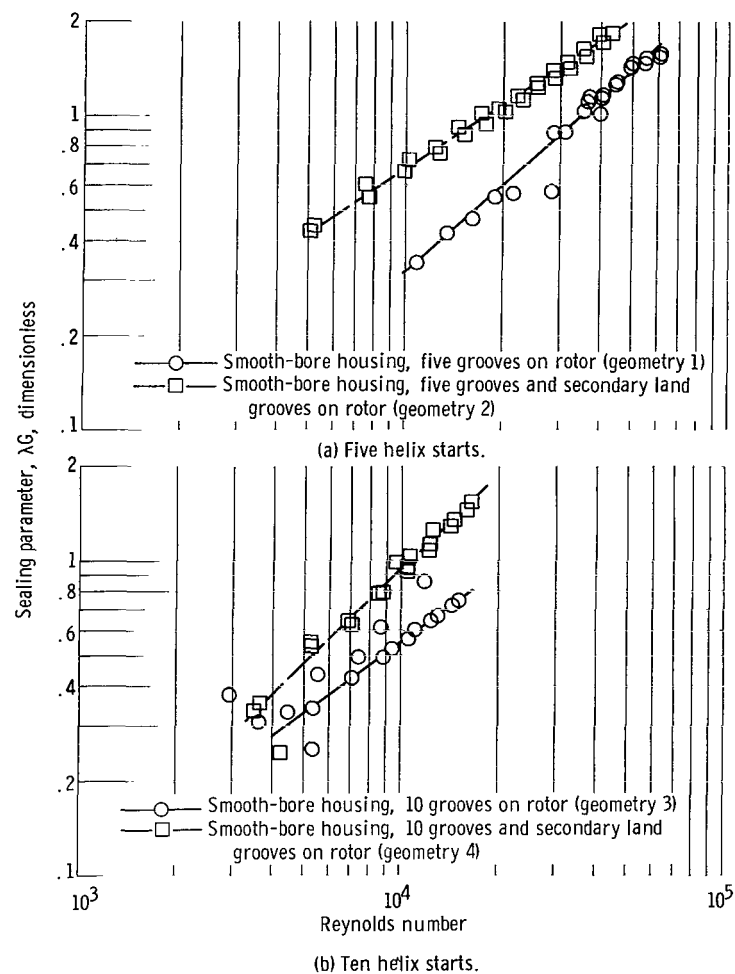


Figure 13. - Comparison of sealing parameter obtained with helically grooved rotor with and without secondary land grooves operating in sodium. Sodium temperature, 165° to 335° C (329° to 635° F).

"The aeronautical and space activities of the United States shall be conducted so as to contribute . . . to the expansion of human knowledge of phenomena in the atmosphere and space. The Administration shall provide for the widest practicable and appropriate dissemination of information concerning its activities and the results thereof."

—NATIONAL AERONAUTICS AND SPACE ACT OF 1958

## NASA SCIENTIFIC AND TECHNICAL PUBLICATIONS

**TECHNICAL REPORTS:** Scientific and technical information considered important, complete, and a lasting contribution to existing knowledge.

**TECHNICAL NOTES:** Information less broad in scope but nevertheless of importance as a contribution to existing knowledge.

**TECHNICAL MEMORANDUMS:** Information receiving limited distribution because of preliminary data, security classification, or other reasons.

**CONTRACTOR REPORTS:** Technical information generated in connection with a NASA contract or grant and released under NASA auspices.

**TECHNICAL TRANSLATIONS:** Information published in a foreign language considered to merit NASA distribution in English.

**TECHNICAL REPRINTS:** Information derived from NASA activities and initially published in the form of journal articles.

**SPECIAL PUBLICATIONS:** Information derived from or of value to NASA activities but not necessarily reporting the results of individual NASA-programmed scientific efforts. Publications include conference proceedings, monographs, data compilations, handbooks, sourcebooks, and special bibliographies.

*Details on the availability of these publications may be obtained from:*

SCIENTIFIC AND TECHNICAL INFORMATION DIVISION  
NATIONAL AERONAUTICS AND SPACE ADMINISTRATION  
Washington, D.C. 20546